Metals **2015**, *5*, 836-849; doi:10.3390/met5020836

OPEN ACCESS

metals

ISSN 2075-4701

www.mdpi.com/journal/metals/

Article

A Mathematical Formulation to Estimate the Effect of Grain Refiners on the Ultimate Tensile Strength of Al-Zn-Mg-Cu Alloys

Halil Ibrahim Kurt [1,*], Murat Oduncuoglu [1,†] and Mehmet Kurt [2,†]

[1] Technical Sciences, University of Gaziantep, Gaziantep 27310, Turkey; E-Mail: oduncuoglu@gmail.com

[2] Department of Metallurgical and Materials Engineering, Engineering Faculty, Fırat University, Elazığ 23119, Turkey; E-Mail: mehmetkurt_27@mynet.com

† These authors contributed equally to this work.

* Author to whom correspondence should be addressed; E-Mail: hiakurt@gmail.com; Tel.: +90-342-360-1171 (ext. 1746); Fax: +90-342-360-1170.

Academic Editor: Hugo F. Lopez

Received: 13 February 2015 / Accepted: 13 May 2015 / Published: 22 May 2015

Abstract: In this study, the feed-forward (FF) neural networks (NNs) with back-propagation (BP) learning algorithm is used to estimate the ultimate tensile strength of unrefined Al-Zn-Mg-Cu alloys and refined the alloys by Al-5Ti-1B and Al-5Zr master alloys. The obtained mathematical formula is presented in great detail. The designed NN model shows good agreement with test results and can be used to predict the ultimate tensile strength of the alloys. Additionally, the effects of scandium (Sc) and carbon (C) rates are investigated by using the proposed equation. It was observed that the tensile properties of Al-Zn-Mg-Cu alloys improved with the addition of 0.5 Sc and 0.01 C wt.%.

Keywords: Al-Zn-Mg-Cu alloys; ultimate tensile strength; modeling; ANN

1. Introduction

Al-Zn-Mg-Cu alloys, using ultra-high strength Al-based alloys, are widely used in aviation, automotive, and aerospace industries due to of their low density, high specific strength, toughness, and fatigue durability [1–7]. The mechanical properties of the alloys can be improved by some important factors such as: minimizing inclusions, applying thermo-mechanical treatments and changing the composition [8]. One of the most important methods to increase the strength is the refining of the grain size, which is described by the well-known Hall-Petch Equation [9]:

$$\sigma_y = \sigma_0 + kd^{-1/2} \tag{1}$$

where σ_y is the yield stress, σ_0 a friction stress, d the grain size and k a constant.

The existing knowledge of grain refinement can be divided into three basic methods: mechanical, chemical, and thermal, whereas the addition of master alloys (chemical) is the most economical one. In the chemical method, the addition of master alloys promotes nucleation and hinders growth [10–14]. Grain refiners used in aluminum (Al) and its alloys are Al-Ti, Al-B, Al-Ti-B, Al-Ti-C, Al-Zr, Al-Sc, and Al-Sr [15–20]. A fine equiaxed grain structure leads to better mechanical properties. Moreover, grain refinement can also bring other advantages, such as enhanced machinability, good surface finish, resistance to hot tearing, high toughness and high yield strength [21,22]. The type and addition level of these master alloys also affect the mechanical properties of alloys. The relation among grain size, changing operation parameters and strength are quite complex and non-linear. Therefore, it is very important to select the correct master alloy to obtain the maximum strength. As an experiment, this phenomenon is costly and time consuming. Therefore, an attempt has been made to model the complex grain refinement phenomena in Al-Zn-Mg-Cu alloys.

Successful modelings of artificial neural networks (ANN) have been reported in materials science [23]. Reddy *et al.* [24] used the feed forward neural network (FFNN) with back-propagation (BP) learning algorithm to predict the grain size as a function of titanium (Ti) and boron (B) addition levels, and holding time during grain refinement of Al–7Si alloy. The authors stated that the grain size of Al–7Si alloy, with good learning precision and generalization, can be predicted with the FFNN model. Rashidi *et al.* [25] modeled the effect of the process parameters, namely current density, saccharin concentration, and bath temperature on the grain size of nano-crystalline nickel coating by using a feed-forwarded multilayer perceptron ANN framework. They reported that there is a remarkable agreement between the model prediction and the experimental observation. Tofigh *et al.* [26] used the FFNN in prediction of hardness, tensile and compressive yield stress, ultimate tensile strength, and elongation percentage of Al alloy reinforced alumina nano-particles. The authors notified that the prediction ability of the model is in good agreement with experimental data.

The aim of this work is to obtain an explicit formulation of the ultimate tensile strength as a function of complex master alloys and, theoretically, to investigate the effect of scandium (Sc) and carbon (C) rates on the ultimate tensile strength of the alloys by using the obtained equation.

2. Background of Neural Networks

ANNs are computationally in the context of artificial intelligence, which is imitating the neural behavior of human beings. ANNs can be called a computer model of the human brain's neural structure. The basic elements of the ANNs are "neurons", which are the processing elements of ANNs. The "network" is defined as the structure in which the neurons act simultaneously in a group. The network involves an input layer, hidden layer, and the output layer [27]. In an ANN, neurons are tightly interconnected in various layers, where the adaptive weights are, conceptually, connection strengths between neurons. The three main characteristics of a NN are weights (w_i), bias (b_i), and transfer function. Each neuron receives inputs, attached with a weight. Each input data is multiplied by the corresponding weight of the neuron connection. Next, a bias value is added to the summation of inputs and corresponding weights (u) according to the following equation:

$$u_i = \sum_{j=1}^{H} w_{ij} x_j + b_i \tag{2}$$

The summation u_i is converted as the output with an activation (transfer) function, $F(u_i)$ yielding a value called the unit's "activation", as the following formula:

$$O = f(u_i) \tag{3}$$

The activation or transfer function that converts a neuron's weighted input to its output activation play the substantial role in the overall performance of an ANN's implementation [28].

3. Neural Network Studies

An extensive literature survey has been performed for available experimental results, as shown Table 1. The addition of grain refiners promotes the formation of fine equiaxed grains by suppressing the growth of columnar and twin columnar grain. The finer grain size also decreases the size of defects, such as micro-pores and second phase particles, thereby contributing to improved mechanical properties [29]. It is clear from Table 1 that the grain refiners and the applied heat treatment result in an increase in the ultimate tensile strength of the alloys. Ebrahimi and Emamy [30] reported that Al-5Ti-1B and Al-5Zr master alloy decreases the grain size of Al-12Zn-3Mg-2.5Cu aluminum alloy, and Al-5Ti-1B master alloy is more effective than Al-5Zr master alloy in reducing the grain size of Al-12Zn-3Mg-2.5Cu aluminum alloy. They expressed that the mechanical properties of the alloy are improved with the addition of grain refiners and heat treatment, and that this improvement can be attributed the increase to nano-metric precipitates, the homogeneity of the microstructure, and the decrease in grain size.

Table 2 shows the change of the input elements, from minimum to maximum, in training and testing sets of NN. The input variables are silicon (Si), magnesium (Mg), zinc (Zn), cupper (Cu), nickel (Ni), iron (Fe), manganese (Mn), chromium (Cr), Ti, zirconium (Zr), Sc, B, C, Al (in wt.%), and heat treatment (HT). The output variable is the ultimate tensile strength (UTS) in MPa. In the program, the alloys with and without heat treatment is coded as "1" and "0", respectively. In ANN system, each input variable is scaled to the range of 0 to 1 by the following the formula:

$$x_N = \frac{x - x_{min.}}{x_{max.} - x_{min.}} \tag{4}$$

where x_N is the normalized value of variable x, and x_{max} and x_{min} are the maximum and minimum values of the variable, respectively.

Table 1. Data set for training and testing.

Ref.	Master Alloys		HT	AGS	UTS
	Type	wt.%		(μm)	(MPa)
Ebrahimi and Emamy [30]	-	-	No	310	328
	-	-	Yes	310	504
	Al-5Ti-1B	0.05	No	38	352
	Al-5Ti-1B	0.05	Yes	38	621
	Al-5Zr	0.3	No	150	328
	Al-5Zr	0.3	Yes	150	530
Fakhraei and Emamy [31]	-	-	No	305	168
	Al-8B	0.1	No	155	190
	Al-8B	0.3	No	130	222
	Al-8B	0.5	No	113	236
	Al-8B	1	No	111	197
	Al-15Zr	0.1	No	215	193
	Al-15Zr	0.3	No	168	226
	Al-15Zr	0.5	No	150	243
	Al-15Zr	1	No	152	202
Fakhraei and Emamy [32]	-	-	No	305	168
	Al-5Ti-1B	0.05	No	178	178
	Al-5Ti-1B	0.1	No	150	183
	Al-5Ti-1B	0.3	No	116	200
	Al-5Ti-1B	0.5	No	100	253
	Al-5Ti-1B	1	No	88	242
Wang *et al.* [33]	-	-	Yes	320	170
	Al-5Ti-1B	0.2	Yes	200	220
	Al-5Ti-1B	0.5	Yes	180	229
	Al-5Ti-1B	1	Yes	100	249
	Al-5Ti-1B	1.5	Yes	80	250
	Al-5Ti-1B	2	Yes	75	241
	Al-5Ti-1B	3	Yes	40	230
	Al-5Ti-1B	5	Yes	70	215
	Al-5Ti-0.25C	0.2	Yes	200	230
	Al-5Ti-0.25C	0.5	Yes	150	260
	Al-5Ti-0.25C	1	Yes	80	267
	Al-5Ti-0.25C	1.5	Yes	65	271
	Al-5Ti-0.25C	2	Yes	40	249
	Al-5Ti-0.25C	3	Yes	50	240
	Al-5Ti-0.25C	5	Yes	80	215
Shabani *et al.* [34]	-	-	Yes	560	260
	Al-5Ti-1B	0.05	Yes	300	283
	Al-5Zr	0.3	Yes	345	276

Table 1. *Cont.*

Ref.	Master Alloys		HT	AGS (μm)	UTS (MPa)
	Type	wt.%			
Ravi *et al.* [29]	-	-	No	630	168
	-	-	No	630	177
	Al-5Ti-1B	2	No	425	189
	Al-1Ti-3B	2	No	215	201
	Al-1Ti-3B	0.5	No	180	227
Kamali *et al.* [35]	-	-	No	190	174
	Al-5Ti-1B	0.05	No	48	217
	Al-5Ti-1B	0.1	No	39	225
	Al-5Ti-1B	0.3	No	41	237
	Al-5Ti-1B	0.5	No	42	245
	Al-5Ti-1B	0.05	Yes	48	318
	Al-5Ti-1B	0.1	Yes	39	330
	Al-5Ti-1B	0.3	Yes	41	350
	Al-5Ti-1B	0.5	Yes	42	354
Wang *et al.* [36]	-	-	No	165	167
	Al-5Ti-1B	0.01	No	87	161
	Al-5Ti-1B	0.02	No	47	183
	Al-5Ti-1B	0.05	No	40	181
	Al-5Ti-1B	0.1	No	52	166
Liu *et al.* [37]	Al-0.04Ti	0.036	No	110	270
	Al-3Sc	0.2	No	172	372
	Al-3Zr+Al-3Sc	0.15+0.2	No	100	393
	Al-0.04Ti+Al-3Zr+Al-3Sc	0.036+0.15+0.2	No	61	395
He *et al.* [38]	-	-	Yes	370	260
	Al-3.8Zr	0.1	Yes	196	272
	Al-3.6Sc	0.2	Yes	370	296
	Al-3.6Sc	0.6	Yes	72	360
	Al-3.8Zr+Al-3.6Sc	0.1+0.2	Yes	42	398

- Any grain refiner was not added in the alloys.

Table 2. Input elements (wt.%).

Elements	Si	Mg	Zn	Cu	Ni	Fe	Mn	Cr	Ti	Zr	Sc	B	C	Al	HT
Min.	0.03	0.02	0	0.03	0	0.15	0	0	0	0	0	0	0	Rem.	No = 0
Max.	13.2	20.4	12.24	4.47	0.95	0.45	0.2	0.1	1	1	0.6	1	0.2		Yes = 1

Output values resulted from ANN are also in the range [0.1], and transformed to their equivalent values, based on a reverse method of the normalization technique [39]. The unnormalized method is as:

$$x = x_N\,(x_{max} - x_{min}) + x_{min} \tag{5}$$

The two main processing phases of NN include training and testing. The training process is the adjustment of weights and biases in order to obtain an output through applying a proper method. Therefore, the experimental results are divided into training and testing sets. The datasets for training and testing are randomly selected from among the experimental results where 61 sets are training set and

6 sets are testing set. It is well known that increasing the data used in the training process of NN enhances its learning ability. Matlab NN toolbox is employed for the network training. Back-propagation (BP) learning algorithm (Levenberg–Marquardt-Trainlm, Boston, MA, USA), the most popular, and an effective, supervised learning method, and sigmoid function, an act activation function that joins curvilinear, linear, and constant behavior, depending on the values of the input, are used for the training of NN [40,41]. Training of the networks starts with adjusting initial random values for weights and biases. After submitting the input vector, forward propagation of the intermediate results leads to the producing of the output vector. Then, the weights and biases would be modified in order to reduce the error. The network replies to an input, without any change in the structure, within the testing process [42,43]. After the network is trained, the testing dataset is used to verify the effectiveness of the network and to estimate the expected performance in the future.

4. Results and Discussion

The main aim is to obtain the explicit formulation of the ultimate tensile strength as a function of input variables. One of the most difficult duties in NN works is the determination of the number of hidden layers and the number of neurons in the hidden layers. It is well known that NNs are typically in layers, which are made up of a number of interconnected nodes that contain an activation function. The input layer, which communicates to one or more hidden layers, where the actual processing is made via a system of weighted connections. The hidden layers then link to an output layer, where the answer is the output [44]. There is no well-defined procedure to find the optimal parameter settings and the network architecture. The trial and error approach is used to determine the number of neurons in the hidden layer. The various neuron numbers in one hidden layer (5–20) are used in this study. It is observed that the optimal architecture of NN with logistic sigmoid transfer function is 15–17–1. The NN toolbox in Matlab is used to obtain the proposed equation. It should be noted that the developed explicit formulation is valid for the ranges of the training set. Additionally, the correlation coefficient of the proposed equation is also evaluated, and is found to be 0.8509. In other words, the average prediction accuracy of the established ANN model is 85.09%.

$$T = 460 \times \dot{T} + 161 \tag{6}$$

where T is ultimate tensile strength and where:

$$\dot{T} = \left(\frac{1}{1+e^{-w}}\right)$$

where:

$$\begin{aligned} w = {} & (0.94889) \times \left(\frac{1}{1+e^{-u1}}\right) + (2.13402) \times \left(\frac{1}{1+e^{-u2}}\right) + (0.45077) \times \left(\frac{1}{1+e^{-u3}}\right) + (-3.32533) \\ & \times \left(\frac{1}{1+e^{-u4}}\right) + (2.39273) \times \left(\frac{1}{1+e^{-u5}}\right) + (-2.47205) \times \left(\frac{1}{1+e^{-u6}}\right) + (0.17732) \\ & \times \left(\frac{1}{1+e^{-u7}}\right) + (1.59606) \times \left(\frac{1}{1+e^{-u8}}\right) + (1.95837) \times \left(\frac{1}{1+e^{-u9}}\right) + (-3.33818) \\ & \times \left(\frac{1}{1+e^{-u10}}\right) + (-0.36762) \times \left(\frac{1}{1+e^{-u11}}\right) + (-2.96723) \times \left(\frac{1}{1+e^{-u12}}\right) + (-2.99594) \\ & \times \left(\frac{1}{1+e^{-u13}}\right) + (-1.59159) \times \left(\frac{1}{1+e^{-u14}}\right) + (-5.78338) \times \left(\frac{1}{1+e^{-u15}}\right) + (-0.19006) \\ & \times \left(\frac{1}{1+e^{-u16}}\right) + (1.50506) * \left(\frac{1}{1+e^{-u17}}\right) + (0.15734) \end{aligned}$$

and

$$u1 = (-0.49993 \times X1) + (-0.00354 \times X2) + (-0.61144 \times X3) + (0.49105 \times X4) + (0.72856 \times X5) + (-0.06895 \times X6) + (-0.03897 \times X7) + (-0.66021 \times X8) + (-0.92799 \times X9) + (0.13060 \times X10) + (0.13452 \times X11) + (0.54220 \times X12) + (0.40258 \times X13) + (0.13213 \times X14) + (0.36274 \times X15) + (-0.23276)$$

$$u2 = (-0.35276 \times X1) + (0.18702 \times X2) + (-0.24048 \times X3) + (1.03259 \times X4) + (0.64191 \times X5) + (-0.32554 \times X6) + (-2.70935 \times X7) + (0.14497 \times X8) + (-1.54846 \times X9) + (1.09702 \times X10) + (-2.60705 \times X11) + (-2.10947 \times X12) + (-0.02828 \times X13) + (-0.29674 \times X14) + (0.09758 \times X15) + (-0.26159)$$

$$u3 = (1.69292 \times X1) + (-0.15616 \times X2) + (0.17488 \times X3) + (-2.36728 \times X4) + (-0.61096 \times X5) + (-2.04671 \times X6) + (0.02049 \times X7) + (0.59184 \times X8) + (0.43818 \times X9) + (-0.31379 \times X10) + (1.14791 \times X11) + (1.12623 \times X12) + (-0.77400 \times X13) + (0.25359 \times X14) + (-1.75379 \times X15) + (-0.15834)$$

$$u4 = (-1.19858 \times X1) + (-0.65841 \times X2) + (1.26693 \times X3) + (-0.12854 \times X4) + (-0.64606 \times X5) + (0.19024 \times X6) + (1.29375 \times X7) + (-0.54070 \times X8) + (-0.85351 \times X9) + (-3.19349 \times X10) + (-1.19332 \times X11) + (-0.36499 \times X12) + (-2.22971 \times X13) + (0.79672 \times X14) + (-0.28841 \times X15) + (-0.05969)$$

$$u5 = (0.31740 \times X1) + (0.23849 \times X2) + (-0.16464 \times X3) + (0.72392 \times X4) + (0.08065 \times X5) + (-0.22394 \times X6) + (-0.45745 \times X7) + (-0.59003 \times X8) + (-0.53258 \times X9) + (-0.09952 \times X10) + (-0.59419 \times X11) + (-0.29143 \times X12) + (-0.45241 \times X13) + (0.52024 \times X14) + (0.60874 \times X15) + (0.58822)$$

$$u6 = (-1.65634 \times X1) + (-0.28557 \times X2) + (0.74052 \times X3) + (-2.75057 \times X4) + (-0.18806 \times X5) + (1.22060 \times X6) + (3.32170 \times X7) + (0.08922 \times X8) + (0.75341 \times X9) + (0.77162 \times X10) + (0.61279 \times X11) + (0.99672 \times X12) + (1.04996 \times X13) + (-1.24403 \times X14) + (-0.36127 \times X15) + (-1.26639)$$

$$u7 = (0.18672 \times X1) + (-0.21317 \times X2) + (-0.06951 \times X3) + (0.23293 \times X4) + (0.18344 \times X5) + (0.86836 \times X6) + (0.15483 \times X7) + (-0.49808 \times X8) + (-0.39467 \times X9) + (0.70716 \times X10) + (0.52081 \times X11) + (-0.15581 \times X12) + (0.04996 \times X13) + (-0.47618 \times X14) + (0.49369 \times X15) + (0.13833)$$

$$u8 = (0.20311 \times X1) + (-0.18870 \times X2) + (0.71925 \times X3) + (0.59576 \times X4) + (0.04333 \times X5) + (-1.38544 \times X6) + (0.22941 \times X7) + (-0.92876 \times X8) + (-0.49392 \times X9) + (-0.35084 \times X10) + (-0.85939 \times X11) + (0.69356 \times X12) + (0.92923 \times X13) + (0.76245 \times X14) + (0.80903 \times X15) + (0.78233)$$

$$u9 = (0.45508 \times X1) + (0.45380 \times X2) + (-0.53263 \times X3) + (0.62014 \times X4) + (0.48778 \times X5) + (-0.42787 \times X6) + (-1.03911 \times X7) + (-0.16981 \times X8) + (0.13517 \times X9) + (2.24826 \times X10) + (-0.05111 \times X11) + (-1.26004 \times X12) + (0.30575 \times X13) + (1.73001 \times X14) + (-0.22815 \times X15) + (0.74025)$$

$$u10 = (-3.04675 \times X1) + (-1.47749 \times X2) + (0.52853 \times X3) + (1.76084 \times X4) + (-1.14597 \times X5) + (4.48201 \times X6) + (0.88897 \times X7) + (-2.78018 \times X8) + (-0.76322 \times X9) + (-1.89132 \times X10) + (-0.37789 \times X11) + (-7.27827 \times X12) + (-0.16189 \times X13) + (1.69861 \times X14) + (-3.22967 \times X15) + (-1.60096)$$

$$u11 = (0.38619 \times X1) + (0.00559 \times X2) + (-0.13668 \times X3) + (-0.13627 \times X4) + (-0.00132 \times X5) + (-0.42122 \times X6) + (0.12256 \times X7) + (0.12089 \times X8) + (0.30673 \times X9) + (-0.19105 \times X10) + (0.09498 \times X11) + (0.33387 \times X12) + (0.13216 \times X13) + (-0.34123 \times X14) + (-0.09914 \times X15) + (-0.47796)$$

$$u12 = (-0.88070 \times X1) + (-1.26162 \times X2) + (1.00008 \times X3) + (0.44580 \times X4) + (-0.69643 \times X5) + (0.54684 \times X6) + (1.47863 \times X7) + (0.26171 \times X8) + (-0.07183 \times X9) + (-2.17460 \times X10) + (1.83544 \times X11) + (-1.22216 \times X12) + (0.19267 \times X13) + (-1.94418 \times X14) + (0.16993 \times X15) + (-0.74403)$$

$$u13 = (-1.16712 \times X1) + (-1.05184 \times X2) + (0.73395 \times X3) + (0.04286 \times X4) + (-0.39426 \times X5) + (2.84218 \times X6) + (1.99864 \times X7) + (-0.22580 \times X8) + (1.15608 \times X9) + (-0.03548 \times X10) + (-1.92515 \times X11) + (-4.03396 \times X12) + (0.38855 \times X13) + (-0.37459 \times X14) + (1.85893 \times X15) + (-0.99138)$$

$$u14 = (-0.04539 \times X1) + (-0.07940 \times X2) + (0.32185 \times X3) + (-0.79070 \times X4) + (-0.20130 \times X5) + (1.03768 \times X6) + (1.17849 \times X7) + (0.17644 \times X8) + (1.38321 \times X9) + (-1.21757 \times X10) + (-1.73489 \times X11) + (-2.77648 \times X12) + (-0.46636 \times X13) + (0.18136 \times X14) + (0.82488 \times X15) + (-0.16546)$$

$$u15 = (-0.97802 \times X1) + (-1.35732 \times X2) + (0.46732 \times X3) + (-1.94090 \times X4) + (0.45079 \times X5) + (0.86831 \times X6) + (0.96056 \times X7) + (0.86766 \times X8) + (-0.27002 \times X9) + (2.17786 \times X10) + (-3.34955 \times X11) + (1.57693 \times X12) + (-0.51299 \times X13) + (1.69850 \times X14) + (-0.16939 \times X15) + (-1.56104)$$

$$u16 = (-0.37956 \times X1) + (-0.13332 \times X2) + (0.05849 \times X3) + (-0.34892 \times X4) + (0.22692 \times X5) + (-0.26460 \times X6) + (-0.97223 \times X7) + (0.30502 \times X8) + (0.22059 \times X9) + (-0.10065 \times X10) + (-0.65479 \times X11) + (0.50434 \times X12) + (-0.54470 \times X13) + (-0.16661 \times X14) + (-0.27592 \times X15) + (-0.04856)$$

$$u17 = (0.18078 \times X1) + (0.16781 \times X2) + (-0.13242 \times X3) + (1.59311 \times X4) + (0.28523 \times X5) + (-0.66845 \times X6) + (-0.07740 \times X7) + (0.03953 \times X8) + (-0.20656 \times X9) + (-0.12734 \times X10) + (-0.86300 \times X11) + (0.42924 \times X12) + (0.24858 \times X13) + (-0.62146 \times X14) + (0.95215 \times X15) + (0.52058)$$

where X1, X2, X3, X4, X5, X6, X7, X8, X9, X10, X11 X12, X13, X14, and X15 are normalized input data of Al, Si, Mg, Zn, Cu, Ni, Fe, Mn, Cr, Ti, Zr, Sc, B, C wt.%, and HT.

Table 3 shows statistical parameters of training and test data sets. The performance of NN is evaluated by the correlation coefficient (R). Mean absolute error (MAE) and mean square error (MSE) are also used as error evaluation criteria in order to facilitate the comparison between predicted values and desired values.

Table 3. Statistical parameters.

Datasets	R	MSE	MAE
Training set	0.985	0.141	2.606
Testing set	0.946	0.528	6.313

The correlation coefficients of training and testing sets are 0.985 and 0.946, respectively, which means that the performance of the NN model is quite high and acceptable. MAE and MSE values for the training set are 2.606 and 0.141, and are 6.313 and 0.528 for testing set. If the MSE reaches zero, the performance of the model is regarded as excellent [45]. It can be said that the proposed NN model is in good agreement with the experimental data, and that all the errors are within acceptable ranges.

Figure 1 illustrates the correlation of NN and test data for the training and testing sets. The "test" means the determined experimental value of UTS and "NN" means the predicted value of UTS by NN, as shown in Figure 1. R^2 values of training and testing are 0.9711 and 0.8946, respectively. R^2 value compares the accuracy of the model to the accuracy of a trivial assessment model. A high R^2 (1) value tells that all points lie exactly on the curve with no scatter, and the results are perfect. It is clear that all the values are higher than 0.89. It can be said that the proposed NN model can predict the ultimate tensile strength of Al-Zn-Mg-Cu alloys with high accuracy and reliability. A few minor deviations between the experimental and theoretical results are observed in the training and testing sets of NN, which can be attributed to the variation in experimental conditions.

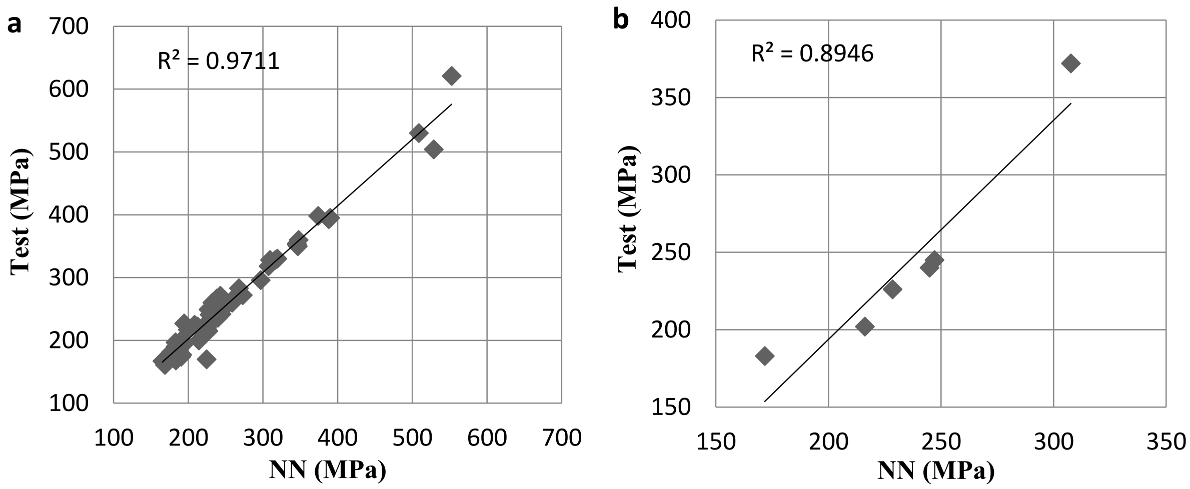

Figure 1. Correlation of NN and Test (**a**) Training set (**b**) Testing set.

One of the most effective elements promoting grain refinement in aluminum alloys is scandium. Aluminum and Al_3Sc have the same lattice structure and the misfit between lattice parameters is about 1.3%. The grain refinement mechanism of primary aluminum with scandium is due to heterogeneous nucleation, and the addition of scandium has been shown to have a beneficial effect on the strength of a cast Al-Mg alloy [46,47]. Figure 2 demonstrates the effect of Sc rates on the ultimate tensile strength of unrefined Al-Zn-Mg-Cu alloys and refined the alloys by Al-5Ti-1B and Al-5Zr using the proposed formulation above (Equation 6). In the case where there is no applied heat treatment, the ultimate tensile strength of Al-Zn-Mg-Cu alloys clearly increases with the addition of Sc. The main reason for this improvement can be attributed to the reduced grain size and the precipitation of more primary complex particles from the melt [48].

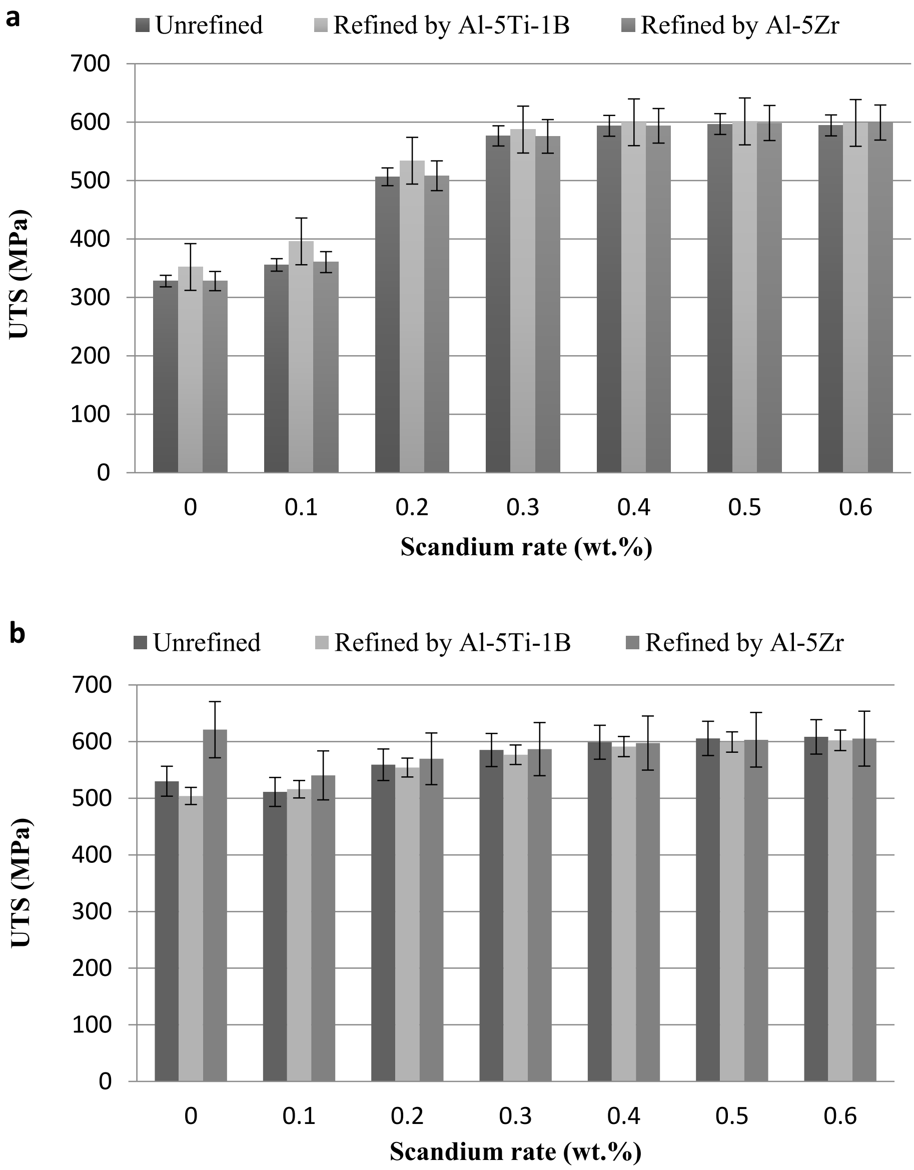

Figure 2. Effect of Sc rate on UTS of Al-Zn-Mg-Cu alloys: (**a**) non heat treatment (**b**) heat treatment.

It is clearly seen that, with the tensile properties of the alloys, first, the applied heat treatment reduces, then increases, the addition of Sc. The comparison of the UTS values revealed that the addition of 0.5% Sc is the most effective method to enhance tensile properties. It is concluded that the ultimate tensile strength of Al-Zn-Mg-Cu alloys, refined by Al-5Ti-1B or Al-5Zr, can be improved with the addition of 0.5% Sc without the need for heat treatment. Figure 3 shows the effect of the rate of C on the ultimate tensile strength of Al-Zn-Mg-Cu alloys containing 0.5 wt.% Sc. It is clear that the ultimate tensile strength of Al-Zn-Mg-Cu alloys, refined by Al-5Zr, enhances with the addition of C to a degree, but that the ultimate tensile strength of unrefined the alloys and refined the alloys by Al-5Ti-1B reduces with the addition of C. The optimum amount of is observed to be 0.01 wt.%.C. It is well known that Al-Ti-C master alloys, which contain $TiAl_3$ and TiC particles, are good refiners for aluminum alloys. These particles in Al-Ti-C master alloys remain stable in the melt and act the active nucleant substrates. These particles very fine and act quickly, but rapidly dissolve in molten aluminum. The morphology, dimension, and distribution of these particles have major impacts on the grain refining efficiency. The homogeneous distribution of these particles increases the mechanical properties of aluminum alloys [49,50].

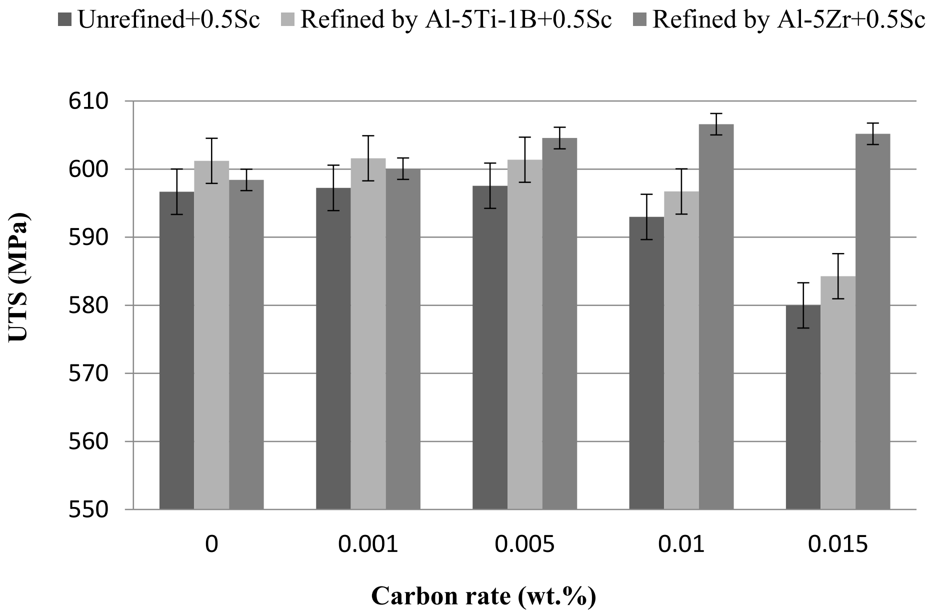

Figure 3. Effect of C rate to UTS of Al-Zn-Mg-Cu alloys.

5. Conclusions

This work proposes an approach for the prediction of ultimate tensile strength of Al-Zn-Mg-Cu alloys refined by Al-5Ti-1B and Al-5Zr. Sixty-seven data are used in this model. Feed-forward NN with back propagation is used for the training process, and the proposed NN model shows good agreement with experimental results. Therefore, the mathematical function is derived in an explicit form by using ANN outputs. The effects of Sc and C on the ultimate tensile strength of Al-Zn-Mg-Cu alloys are predicted with a high success rate. It is suggested that the strength of the alloys, refined by Al-5Ti-1B or Al-5Zr, can be increased with the addition of 0.5% Sc without heat treatment. All R and R^2 values for training, testing, and formula are larger than 0.94 and 89, respectively. This notes that the composed prediction model has a high reliability rate. The mean absolute error for the predicted values does not exceed 6.4%. Hence, it can be concluded that considerable savings, in terms of cost and time, could be obtained by using the advanced neural network model.

Author Contributions

All authors contributed equally to this work. All authors analyzed and interpreted the data, discussed the conclusions, and prepared the manuscript.

Conflicts of Interest

The authors declare no conflicts of interest.

References

1. Fan, X.; Jiang, D.; Meng, Q.; Zhong, L. The microstructural evolution of an Al–Zn–Mg–Cu alloy during homogenization. *Mater. Lett.* **2006**, *60*, 1475–1479.
2. Chen, J.-Z.; Zhen, L.; Yang, S.-J.; Dai, S.-L. Effects of precipitates on fatigue crack growth rate of aa 7055 aluminum alloy. *Trans. Nonferrous Met. Soc. China* **2010**, *20*, 2209–2214.
3. Wang, S.C.; Starink, M.J.; Gao, N. Precipitation hardening in Al–Cu–Mg alloys revisited. *Scr. Mater.* **2006**, *54*, 287–291.
4. Miller, W.S.; Zhuang, L.; Bottema, J.; Wittebrood, A.J.; de Smet, P.; Haszler, A.; Vieregge, A. Recent development in aluminium alloys for the automotive industry. *Mater. Sci. Eng. A* **2000**, *280*, 37–49.
5. Cui, J.; Roven, H.J. Recycling of automotive aluminum. *Trans. Nonferrous Met. Soc. China* **2010**, *20*, 2057–2063.
6. Rendigs, K. Aluminium structures used in aerospace-status and prospects. *Mater. Sci. Forum* **1997**, *242*, 11–24.
7. Williams, J.C.; Starke, E.A., Jr. Progress in structural materials for aerospace systems1. *Acta Mater.* **2003**, *51*, 5775–5799.
8. Srivatsan, T.S.; Sriram, S.; Veeraraghavan, D.; Vasudevan, V.K. Microstructure, tensile deformation and fracture behaviour of aluminium alloy 7055. *J. Mater. Sci.* **1997**, *32*, 2883–2894.
9. Hall, E. The deformation and ageing of mild steel: III discussion of results. *Proc. Phys. Soc. Sect. B* **1951**, *64*, 747.
10. McCartney, D. Grain refining of aluminium and its alloys using inoculants. *Int. Mater. Rev.* **1989**, *34*, 247–260.
11. Campbell, J. Effects of vibration during solidification. *Int. Met. Rev.* **1981**, *26*, 71–108.
12. Chalmers, B. *Principles of Solidification*; John Wiley and Sons, Inc.: New York, NY, USA, 1964.
13. Easton, M.; StJohn, D. Grain refinement of aluminum alloys: Part I. The nucleant and solute paradigms—A review of the literature. *Metall. Mat. Trans. A* **1999**, *30*, 1613–1623.
14. Jiang, K.; Liu, X. The effect of melting temperature and time on the TiC particles. *J. Alloy. Compd.* **2009**, *484*, 95–101.
15. Li, P.; Kandalova, E.G.; Nikitin, V.I. Grain refining performance of Al–Ti master alloys with different microstructures. *Mater. Lett.* **2005**, *59*, 723–727.
16. Wang, T.; Chen, Z.; Fu, H.; Gao, L.; Li, T. Grain refinement mechanism of pure aluminum by inoculation with Al–B master alloys. *Mater. Sci. Eng.: A* **2012**, *549*, 136–143.
17. Wang, T.; Fu, H.; Chen, Z.; Xu, J.; Zhu, J.; Cao, F.; Li, T. A novel fading-resistant Al–3Ti–3B grain refiner for Al–Si alloys. *J. Alloy. Compd.* **2012**, *511*, 45–49.
18. Liu, X.; Wang, Z.; Zang, Z.; Bian, X. The relationship between microstructures and refining performances of Al–Ti–C master alloys. *Mater. Sci. Eng.: A* **2002**, *332*, 70–74.

19. Li, B.; Pan, Q.; Huang, X.; Yin, Z. Microstructures and properties of Al–Zn–Mg–Mn alloy with trace amounts of sc and zr. *Mater. Sci. Eng.: A* **2014**, *616*, 219–228.
20. Yang, M.-B.; Pan, F.-S.; Cheng, R.-J.; Tang, A.-T. Effects of Al-10Sr master alloys on grain refinement of AZ31 magnesium alloy. *Trans. Nonferrous Met. Soc. China* **2008**, *18*, 52–58.
21. Birol, Y. Production of Al–Ti–B master alloys from ti sponge and kbf4. *J. Alloy. Compd.* **2007**, *440*, 108–112.
22. Wróbel, T. Review of inoculation methods of pure aluminium primary structure. *Arch. Mater. Sci. Eng.* **2011**, *50*, 110–119.
23. Kurt, H.I.; Oduncuoglu, M. Formulation of the effect of different alloying elements on the tensile strength of the *in situ* Al-Mg_2si composites. *Metals* **2015**, *5*, 371–382.
24. Reddy, N.S.; Rao, A.K.P.; Chakraborty, M.; Murty, B.S. Prediction of grain size of Al–7Si alloy by neural networks. *Mater. Sci. Eng. A* **2005**, *391*, 131–140.
25. Rashidi, A.M.; Eivani, A.R.; Amadeh, A. Application of artificial neural networks to predict the grain size of nano-crystalline nickel coatings. *Comput. Mater. Sci.* **2009**, *45*, 499–504.
26. Tofigh, A.A.; Rahimipour, M.R.; Shabani, M.O.; Alizadeh, M.; Heydari, F.; Mazahery, A.; Razavi, M. Optimized processing power and trainability of neural network in numerical modeling of al matrix nano composites. *J. Manuf. Process.* **2013**, *15*, 518–523.
27. Yurdakul, M.; Akdas, H. Modeling uniaxial compressive strength of building stones using non-destructive test results as neural networks input parameters. *Constr. Build. Mater.* **2013**, *47*, 1010–1019.
28. Jaiswal, S.; Benson, E.R.; Bernard, J.C.; van Wicklen, G.L. Neural network modelling and sensitivity analysis of a mechanical poultry catching system. *Biosyst. Eng.* **2005**, *92*, 59–68.
29. Ravi, K.R.; Manivannan, S.; Phanikumar, G.; Murty, B.S.; Sundarraj, S. Influence of Mg on grain refinement of near eutectic Al-Si alloys. *Metall. Mat. Trans. A* **2011**, *42*, 2028–2039.
30. Seyed Ebrahimi, S.H.; Emamy, M. Effects of Al–5Ti–1B and Al–5Zr master alloys on the structure, hardness and tensile properties of a highly alloyed aluminum alloy. *Mater. Des.* **2010**, *31*, 200–209.
31. Fakhraei, O.; Emamy, M. Effects of Zr and B on the structure and tensile properties of Al–20% Mg alloy. *Mater. Des.* **2014**, *56*, 557–564.
32. Fakhraei, O.; Emamy, M.; Farhangi, H. The effect of Al–5Ti–1B grain refiner on the structure and tensile properties of Al–20%Mg alloy. *Mater. Sci. Eng. A* **2013**, *560*, 148–153.
33. Wang, E.; Gao, T.; Nie, J.; Liu, X. Grain refinement limit and mechanical properties of 6063 alloy inoculated by Al–Ti–C (B) master alloys. *J. Alloy. Compd.* **2014**, *594*, 7–11.
34. Shabani, M.J.; Emamy, M.; Nemati, N. Effect of grain refinement on the microstructure and tensile properties of thin 319 Al castings. *Mater. Des.* **2011**, *32*, 1542–1547.
35. Kamali, H.; Emamy, M.; Razaghian, A. The influence of Ti on the microstructure and tensile properties of cast Al–4.5Cu–0.3Mg alloy. *Mater. Sci. Eng.: A* **2014**, *590*, 161–167.
36. Wang, D.; de Cicco, M.P.; Li, X. Using diluted master nanocomposites to achieve grain refinement and mechanical property enhancement in as-cast Al–9Mg. *Mater. Sci. Eng.: A* **2012**, *532*, 396–400.
37. Liu, Z.; Li, Z.; Wang, M.; Weng, Y. Effect of complex alloying of Sc, Zr and Ti on the microstructure and mechanical properties of Al–5Mg alloys. *Mater. Sci. Eng.: A* **2008**, *483–484*, 120–122.

38. He, Y.-D.; Zhang, X.-M.; You, J.-H. Effect of minor Sc and Zr on microstructure and mechanical properties of Al-Zn-Mg-Cu alloy. *Trans. Nonferrous Met. Soc. China* **2006**, *16*, 1228–1235.
39. Hassan, A.M.; Alrashdan, A.; Hayajneh, M.T.; Mayyas, A.T. Prediction of density, porosity and hardness in aluminum–copper-based composite materials using artificial neural network. *J. Mater. Process. Technol.* **2009**, *209*, 894–899.
40. Cevik, A.; Kutuk, M.A.; Erklig, A.; Guzelbey, I.H. Neural network modeling of arc spot welding. *J. Mater. Process. Technol.* **2008**, *202*, 137–144.
41. Rumelhart, D.E.; Hinton, G.E.; Williams, R.J. Learning internal representations by error propagation. In *Parallel Distributed Processing: Explorations in the Microstructure of Cognition*; David, E.R., James, L.M., Group, C.P.R., Eds.; MIT Press: Cambridge, MA, USA, 1986; Volume 1, pp. 318–362.
42. Prasad, B.K.R.; Eskandari, H.; Reddy, B.V.V. Prediction of compressive strength of scc and hpc with high volume fly ash using ann. *Constr. Build. Mater.* **2009**, *23*, 117–128.
43. Shafabakhsh, G.H.; Ani, O.J.; Talebsafa, M. Artificial neural network modeling (ANN) for predicting rutting performance of nano-modified hot-mix asphalt mixtures containing steel slag aggregates. *Constr. Build. Mater.* **2015**, *85*, 136–143.
44. Pandit, S.; Mandal, C.; Patra, A. *Nano-Scale Cmos Analog Circuits: Models and Cad Techniques for High-Level Design*; CRC Press: Boca Raton, FL, USA, 2014.
45. Sun, Y.; Zeng, W.D.; Zhang, X.M.; Zhao, Y.Q.; Ma, X.; Han, Y.F. Prediction of tensile property of hydrogenated Ti600 titanium alloy using artificial neural network. *J. Mater. Eng. Perform.* **2011**, *20*, 335–340.
46. Davydov, V.G.; Rostova, T.D.; Zakharov, V.V.; Filatov, Y.A.; Yelagin, V.I. Scientific principles of making an alloying addition of scandium to aluminium alloys. *Mater. Sci. Eng. A* **2000**, *280*, 30–36.
47. Lathabai, S.; Lloyd, P.G. The effect of scandium on the microstructure, mechanical properties and weldability of a cast Al–Mg alloy. *Acta Mater.* **2002**, *50*, 4275–4292.
48. Norman, A.F.; Hyde, K.; Costello, F.; Thompson, S.; Birley, S.; Prangnell, P.B. Examination of the effect of Sc on 2000 and 7000 series aluminium alloy castings: For improvements in fusion welding. *Mater. Sci. Eng. A* **2003**, *354*, 188–198.
49. Ding, H.; Li, H.; Liu, X. Different elements-induced destabilisation of TiC and its application on the grain refinement of mg–al alloys. *J. Alloy. Compd.* **2009**, *485*, 285–289.
50. Quested, T.E.; Greer, A.L. The effect of the size distribution of inoculant particles on as-cast grain size in aluminium alloys. *Acta Mater.* **2004**, *52*, 3859–3868.